

# KummerU clutter model for PolSAR data: Application to segmentation and classification

Lionel Bombrun, Gabriel Vasile, Michel Gay, Frédéric Pascal, Jean-Philippe Ovarlez

### ▶ To cite this version:

Lionel Bombrun, Gabriel Vasile, Michel Gay, Frédéric Pascal, Jean-Philippe Ovarlez. KummerU clutter model for PolSAR data: Application to segmentation and classification. SONDRA - 2nd SONDRA Workshop, May 2010, Cargèse, France. pp.4. hal-00488337

HAL Id: hal-00488337

https://hal.science/hal-00488337

Submitted on 1 Jun 2010

**HAL** is a multi-disciplinary open access archive for the deposit and dissemination of scientific research documents, whether they are published or not. The documents may come from teaching and research institutions in France or abroad, or from public or private research centers. L'archive ouverte pluridisciplinaire **HAL**, est destinée au dépôt et à la diffusion de documents scientifiques de niveau recherche, publiés ou non, émanant des établissements d'enseignement et de recherche français ou étrangers, des laboratoires publics ou privés.

## KUMMERU CLUTTER MODEL FOR POLSAR DATA: APPLICATION TO SEGMENTATION AND CLASSIFICATION

L. Bombrun<sup>1,2</sup>, G. Vasile<sup>1</sup>, M. Gay<sup>1</sup>, F. Pascal<sup>2</sup> and J.-P. Ovarlez<sup>2,3</sup>

<sup>1</sup>: Grenoble-Image-sPeach-Signal-Automatics Lab, CNRS / Grenoble-INP, FRANCE,

{lionel.bombrun|gabriel.vasile|michel.gay}@gipsa-lab.grenoble-inp.fr

<sup>2</sup>: SONDRA, Supélec, FRANCE, frederic.pascal@supelec.fr

<sup>3</sup>: French Aerospace Lab, ONERA DEMR/TSI, FRANCE, ovarlez@onera.fr

#### **ABSTRACT**

In this paper, Spherically Invariant Random Vectors (SIRV) are introduced to describe the heterogeneity of the Polarimetric Synthetic Aperture Radar (PolSAR) clutter. In this context, the scalar texture parameter and the normalized covariance matrix are extracted from the PolSAR images. If the texture parameter is modeled by a Fisher Probability Density Function (PDF), the observed target scattering vector follows a KummerU PDF. This PDF is then implemented in a hierarchical segmentation algorithm. Finally, segmentation results are shown on both synthetic and real images.

*Index Terms*— Fisher PDF, KummerU PDF, PolSAR data, Segmentation, Spherically Invariant Random Vectors.

#### 1. INTRODUCTION

Because of its all weather and all-day monitoring capabilities, Synthetic Aperture Radar (SAR) imagery has been widely used for global Earth monitoring. Such systems offer a number of advantages for Earth-surface and feature observation compared to optical sensors. For low resolution images, the classical Wishart distribution has been successfully validated in classification and segmentation of PolSAR data [1] [2]. With the new generation of high resolution SAR sensors, high quality images of the Earth's surface are acquired. They offer the opportunity to observe thinner spatial features from space. Nevertheless, with such sensors, only a small number of scatterers are present in each resolution cell. Classical statistical models can therefore been reconsidered.

To overcome this difficulty, Anfinsen *et al.* [3] have introduced the Relaxed Wishart distribution, which have shown promising results to model forested scenes. Other heterogeneous clutter models have been proposed in the literature by means of the Spherically Invariant Random Vectors.

#### 2. KUMMERU HETEROGENEOUS CLUTTER

In PolSAR imagery, the target vector  $\mathbf{k}$  is a complex vector of length p, and could be written under the SIRV model hy-

pothesis as (1). It is defined as the product of a square root of a positive random variable  $\tau$  (representing the texture) with an independent circular complex Gaussian vector  $\mathbf{z}$  with zero mean and covariance matrix  $[M] = E\{\mathbf{z}\mathbf{z}^H\}$  (representing the speckle):

$$\mathbf{k} = \sqrt{\tau} \mathbf{z} \tag{1}$$

where the superscript H denotes the complex conjugate transposition and  $E\{\cdot\}$  the mathematical expectation.

SIRV representation is not unique, a normalization condition is necessary. Indeed, if  $[M_1]$  and  $[M_2]$  are two covariances matrices such that  $[M_1] = \alpha[M_2]$  with  $\alpha \in \mathbb{R}^{+*}$ . Then  $\{\tau_1, [M_1]\}$  and  $\{\tau_2 = \tau_1/\alpha, [M_2]\}$  describe the same SIRV. In this paper, the trace of the covariance matrix is normalized to p the dimension of target scattering vector.

For a given covariance matrix [M], the Maximum Likelihood (ML) estimator of the texture for the pixel i ( $\tau_i$ ) is given by:

$$\hat{\tau}_i = \frac{\mathbf{k}_i^H [M]^{-1} \mathbf{k}_i}{p}.$$
 (2)

where p is the dimension of the target scattering vector  $\mathbf{k}$  (p=3 for the reciprocal case).

The ML estimator of the normalized covariance matrix under the deterministic texture case is the solution of the following recursive equation:

$$[\hat{M}]_{FP} = \frac{p}{N} \sum_{i=1}^{N} \frac{\mathbf{k}_i \mathbf{k}_i^H}{\mathbf{k}_i^H [\hat{M}]_{FP}^{-1} \mathbf{k}_i} \quad \text{with} \quad Tr([\hat{M}]_{FP}) = p$$
(3)

Pascal *et al.* have established the existence and the uniqueness, up to a scalar factor, of the Fixed Point estimator of the normalized covariance matrix, as well as the convergence of the recursive algorithm whatever the initialization [4] [5].

When the texture is assumed to be deterministic, the ML estimator of the normalized covariance matrix is given by  $\hat{M}_{FP}$  in (3). But, when the texture is a random variable,  $\hat{M}_{FP}$  is not the ML estimator, it is an "approximate" ML estimator. The ML estimator of the normalized covariance matrix depends on the texture PDF  $p_{\tau}(\tau)$ , its expression is linked with

the density generator function  $h_p(x)$  by :

$$[\hat{M}_{ML}] = \frac{1}{N} \sum_{i=1}^{N} \frac{h_{p+1} \left( \mathbf{k}_{i}^{H} [\hat{M}_{ML}]^{-1} \mathbf{k}_{i} \right)}{h_{p} \left( \mathbf{k}_{i}^{H} [\hat{M}_{ML}]^{-1} \mathbf{k}_{i} \right)} \mathbf{k}_{i} \mathbf{k}_{i}^{H}$$
(4)

where:

$$h_p(x) = \int_0^{+\infty} \frac{1}{\tau^p} \exp\left(-\frac{x}{\tau}\right) p_\tau(\tau) d\tau \tag{5}$$

#### 2.1. Scalar texture modeling

#### 2.1.1. Fisher PDF

The Fisher distribution is known as the type VI solution of the Pearson system. Its PDF is defined by three parameters as [6]:

$$\mathcal{F}\left[\tau|m,\mathcal{L},\mathcal{M}\right] = \frac{\Gamma(\mathcal{L}+\mathcal{M})}{\Gamma(\mathcal{L})\Gamma(\mathcal{M})} \frac{\mathcal{L}}{\mathcal{M}m} \frac{\left(\frac{\mathcal{L}\tau}{\mathcal{M}m}\right)^{\mathcal{L}-1}}{\left(1 + \frac{\mathcal{L}\tau}{\mathcal{M}m}\right)^{\mathcal{L}+\mathcal{M}}} \quad (6)$$

with  $\mathcal{L}>0$  and  $\mathcal{M}>0$ . m is a scale parameter.  $\mathcal{L}$  and  $\mathcal{M}$  are two shape parameters which control the behaviour of the Fisher PDF between an heavy head (Gamma PDF) and an heavy tail (Inverse Gamma PDF) distribution. Low values of shape parameters leads to a significant texture.

#### 2.1.2. Benefit of Fisher PDF

To evaluate the potential and limits of Fisher PDFs to model the texture of PolSAR images, four data-set at X-, C-, L- and P-bands are analyzed. From those data-set, the covariance matrix  $[M]_{FP}$  and texture parameter  $\tau$  are estimated on a sliding  $7 \times 7$  window according to (2) and (3). Then, the second ( $\kappa_2$ ) and third ( $\kappa_3$ ) log-cumulant of the texture parameter are computed. Table 1 shows the percentage of points which belong respectively to the Beta, Inverse Beta and Fisher PDF domain definition in the  $\kappa_2/\kappa_3$  plan representation [6].

It yields that, for the four studied data-set, at least 75% of the data belongs to the Fisher  $\kappa_2/\kappa_3$  domain. The other amount of points which does not satisfy the Fisher model are due to both estimation errors (log-cumulants  $\kappa_2$  and  $\kappa_3$  are computed on a sliding  $7\times 7$  square window) and real data properties. It shows that Fisher PDFs can be suitable to model the scalar texture parameter of PolSAR data.

#### 2.2. The KummerU PDF

For a Fisher distributed texture, the target scattering vector PDF has been mathematically established [7] [8]:

$$p_{\mathbf{k}}(\mathbf{k}) = \frac{1}{\pi^p |[M]|} \frac{\Gamma(\mathcal{L} + \mathcal{M})}{\Gamma(\mathcal{L})\Gamma(\mathcal{M})} \left(\frac{\mathcal{L}}{\mathcal{M}m}\right)^p \Gamma(p + \mathcal{M}) U(a; b; z)$$
(7)

**Table 1**. Texture modeling in the  $\kappa_2/\kappa_3$  plan.

	RAMSES	CONVAIR	ESAR	RAMSES
Data set	Brétigny	Ottawa	Oberpfaffenhofen	Nezer
	X-band	C-band	L-band	P-band
$p_{\mathrm{Fisher}}$	81.93%	95.76%	92.46%	75.59%
$p_{ m Beta}$	16.72%	3.61%	6.31%	24.35%
p <sub>Inverse Beta</sub>	1.35%	0.63%	1.23%	0.06%

with  $a = p + \mathcal{M}$ ,  $b = 1 + p - \mathcal{L}$  and  $z = \frac{\mathcal{L}}{\mathcal{M}m}\mathbf{k}^H[M]^{-1}\mathbf{k}$ .  $|\cdot|$  and  $U(\cdot;\cdot;\cdot)$  denote respectively the determinant operator and the confluent hypergeometric function of the second kind (KummerU). In the following, this multivariate distribution is named the KummerU PDF.

For a KummerU distributed clutter, the expression of the ML estimator of the covariance matrix has been mathematically established. It yields [8]:

$$[\hat{M}_{ML}] = \frac{p + \mathcal{M}}{N} \left( \frac{\mathcal{L}}{\mathcal{M}m} \right)$$

$$\times \sum_{i=1}^{N} \frac{U\left(p + 1 + \mathcal{M}; 2 + p - \mathcal{L}; \frac{\mathcal{L}}{\mathcal{M}m} \mathbf{k}_{i}^{H} [\hat{M}_{ML}]^{-1} \mathbf{k}_{i}\right)}{U\left(p + \mathcal{M}; 1 + p - \mathcal{L}; \frac{\mathcal{L}}{\mathcal{M}m} \mathbf{k}_{i}^{H} [\hat{M}_{ML}]^{-1} \mathbf{k}_{i}\right)} \mathbf{k}_{i} \mathbf{k}_{i}^{H}$$
(8)

#### 3. HIERARCHICAL SEGMENTATION

In this section, a segmentation application of the new multivariate KummerU PolSAR model is proposed. The hierarchical segmentation algorithm proposed by Beaulieu and Touzi [9] is adapted to the KummerU distributed target scattering vector. The segmentation algorithm is a classical iterative merge algorithm. At each iteration, the two 4-connex segments (regions) which minimize the Stepwise Criterion (SC) are merged. A 4-connex segments pair is a group of two segments where at least one pixel of the first segment is in the neighbourhood of one pixel of the second segment with the 4-connexity sense.

#### 3.1. Similarity measure

At each iteration, merging two segments yields a decrease in the log-likelihood function. The stepwise criterion is based on this consideration. The hierarchical segmentation algorithm merges the two adjacent segments  $S_i$  and  $S_j$  which minimizes the loss of likelihood of the partition (which is defined as the sum of likelihoods of partition's segments). The stepwise criterion ( $SC_{i,j}$ ) can be expressed as [9]:

$$SC_{i,j} = MLL(S_i) + MLL(S_j) - MLL(S_i \cup S_j)$$
 (9)

where  $MLL(\cdot)$  denotes the segment maximum log-likelihood function. It is the log-likelihood of the segment with respect

to the assumed probability density function (for example, the KummerU distribution) whose parameters are estimated in the maximum likelihood sense. Its expression is given by:

$$MLL(S) = \sum_{i \in S} \ln \left( p_{\mathbf{k}}(\mathbf{k}_i | \theta_S) \right)$$
 (10)

 $\theta_S$  represents the set of distribution parameters.

#### 3.1.1. For the KummerU PDF

In general, the covariance matrix and texture parameters are unknown. One solution consists in replacing the SIRV parameters by their estimates. After replacing the covariance matrix [M] and texture parameters  $(m, \mathcal{L} \text{ and } \mathcal{M} \text{ for the Fisher PDF})$  by their respective ML estimators, the Generalized Maximum Log-Likelihood (GMLL) becomes:

$$GMLL(S) = -pN \ln(\pi) - N \ln \left\{ |[\hat{M}_{ML}]| \right\}$$

$$+N \ln \left\{ \frac{\Gamma(\hat{\mathcal{L}} + \hat{\mathcal{M}}) \Gamma(p + \hat{\mathcal{M}})}{\Gamma(\hat{\mathcal{L}}) \Gamma(\hat{\mathcal{M}})} \right\} + pN \ln \left\{ \frac{\hat{\mathcal{L}}}{\hat{\mathcal{M}}\hat{m}} \right\}$$

$$+ \sum_{i \in S} \ln \left\{ U \left( p + \hat{\mathcal{M}}; 1 + p - \hat{\mathcal{L}}; \frac{\hat{\mathcal{L}}}{\hat{\mathcal{M}}\hat{m}} \mathbf{k}_i^H [\hat{M}_{ML}]^{-1} \mathbf{k}_i \right) \right\}$$
(11)

where  $\hat{\mathcal{L}}$ ,  $\hat{\mathcal{M}}$  and  $\hat{m}$  are respectively the ML estimators of the Fisher parameters  $\mathcal{L}$ ,  $\mathcal{M}$  and m.  $[\hat{M}_{ML}]$  is the ML estimator of  $[M_{ML}]$  for segment S (4).

It can be noticed that the second term of (11) corresponds to the Wishart criterion [9]. All other terms can be viewed as correction terms introduced by the texture modeling of Pol-SAR data.

#### 3.2. Segmentation results

To evaluate the potential and limits of the method, the hierarchical segmentation algorithm proposed by Beaulieu and Touzi [9] has been implemented. Fig. 1 shows the standard deviation for the normalized KummerU criterion (SC/N) as a function of the window size N. This curve has been plotted for two regions containing KummerU realizations with two different set of parameters. As observed in Fig. 1, the standard deviation is stable for sufficiently large region. For segments containing less than 50 pixels, the standard deviation increases, probably due to a poor parameter estimation. It yields that a reasonable 'minimum window' for the KummerU criterion should contain at least 50 pixels.

In the following the Gaussian and KummerU segmentation are tested with both synthetic and high resolution SLC images.

#### 3.2.1. On a synthetic image

The synthetic data-set consists of an image of  $140 \times 140$  pixels. It is composed of six areas. Five of them contain in-

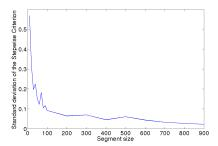


**Fig. 1**. Standard deviation of the normalized KummerU stepwise criterion as a function of the window size N.

dependent realizations of the multivariate KummerU distribution (7). The outer area (class 1) is a special case, since its texture is deterministic and constant (equals 1). It follows that pixels in this area are drawn from a multivariate Gaussian PDF. It can also be viewed as a KummerU PDF with infinite shape parameters  $\mathcal L$  and  $\mathcal M$ .

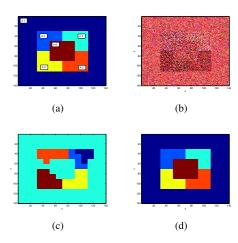


**Fig. 2**. Segmentation results of a simulated data-set  $(140 \times 140 \text{ pixels})$ . (a) Ground truth. (b) Colored composition of the target vector in the Pauli basis  $[k]_1$ - $[k]_3$ - $[k]_2$ . Partitions containing 6 segments: (c) Gaussian criterion and (d) KummerU criterion.

The Gaussian distribution can be viewed as a particular case of the KummerU distribution (for large shape parameters  $\mathcal{L}$  and  $\mathcal{M}$ ). It is expected that the KummerU segmentation gives at least the same performances as the Gaussian criterion. The hierarchical segmentation algorithm is initialized with a partition where each segment is a bloc of  $10 \times 10$  pixels. The initial partition is composed by 196 segments. Segmentation results based on the Gaussian and KummerU criteria are respectively shown on Fig. 2(c) and Fig. 2(d) with partitions containing 6 segments.

For the Gaussian criterion, only the determinant of the sample covariance matrix is taken into account. Both the structure of the covariance matrix and the power (texture) of the clutter are ignored. Consequently, the Gaussian criterion cannot distinguish between two regions having different texture values and/or covariance matrices whose determinants are equals, but having different structure. The KummerU criterion uses information about the texture and full information about the covariance matrix, and is able to give a better segmentation of heterogeneous scenes.

#### 3.2.2. On very high resolution X-band data

In this section, a very high resolution data-set acquired by the X-band RAMSES sensor over the Salon de Provence test-site with a resolution of 10cm is analyzed. Fig. 3(a) shows an optical image of the test-site. Segmentation results with the Gaussian and KummerU criteria are respectively shown in Fig. 3(b) and Fig. 3(c). The segmentation algorithm is initialized with a partition where each segment is a bloc of  $7 \times 7$  pixels.

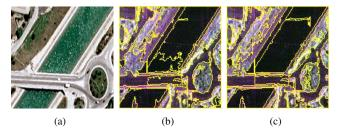


**Fig. 3.** Segmentation results for the X-band RAMSES data over the Salon de Provence test-site ( $1050 \times 1050$  pixels). Partitions containing 55 segments over a colored composition of the target vector in the Pauli basis  $[k]_2$ - $[k]_3$ - $[k]_1$ : (a) Optical image ©CNES/Spot-Image, (b) Gaussian criterion, (c) KummerU criterion.

From this data-set, it can be noticed that more features are segmented in the traffic circle with the KummerU criterion than with the Gaussian criterion. Moreover, the artifact in the water (on the North East of the image) is better retrieved with the KummerU segmentation. Concerning the water itself, the Gaussian criterion leads to an over-segmented partition, especially near the bridge.

#### 4. CONCLUSION

In this paper, authors have proposed to apply the SIRV estimation scheme to derive the covariance matrix and the texture parameter. If the texture parameter  $\tau$  is Fisher distributed, the target scattering vector follows a KummerU PDF. Then, this distribution has been implemented in a ML hierarchical segmentation algorithm. Segmentation results on a very high resolution PolSAR data have shown that the SIRV estimation scheme combined with the KummerU PDF provide the best performances compared to the classical Gaussian hypothesis.

Further works will deal with the use of multivariate statistics for clutter modeling, with an application of change detection in PolSAR imagery.

#### 5. ACKNOWLEDGMENT

The authors would also like to thank the French Aerospace Lab (ONERA) for providing the very high resolution PolSAR images.

#### 6. REFERENCES

- [1] J.S. Lee, M.R. Grunes, T.L. Ainsworth, L.J. Du, D.L. Schuler, and S.R. Cloude, "Unsupervised Classification Using Polarimetric Decomposition and the Complex Wishart Classifier," *IEEE Transactions on Geoscience and Remote Sensing*, vol. 37, no. 5, pp. 2249–2258, 1999.
- [2] H. Skriver, J. Schou, A.A. Nielsen, and K. Conradsen, "Polarimetric Segmentation using the Comple Wishart Test Statistic," in *Geoscience and Remote Sensing, IGARSS '02, Toronto, Canada*, 2002, vol. 2, pp. 1011–1013.
- [3] S.N. Anfinsen, T. Eltoft, and A.P. Doulgeris, "A Relaxed Wishart Model for Polarimetric SAR Data," in *PolInSAR*, *Frascati*, *Italy*, 2009.
- [4] F. Pascal, Y. Chitour, J. P. Ovarlez, P. Forster, and P. Larzabal, "Covariance Structure Maximum-Likelihood Estimates in Compound Gaussian Noise: Existence and Algorithm Analysis," *IEEE Transactions on Signal Processing*, vol. 56, no. 1, pp. 34–48, 2008.
- [5] F. Pascal, P. Forster, J. P. Ovarlez, and P. Larzabal, "Performance Analysis of Covariance Matrix Estimates in Impulsive Noise," *IEEE Transactions on Signal Processing*, vol. 56, no. 6, pp. 2206–2216, 2008.
- [6] J-M. Nicolas, "Application de la Transformée de Mellin: Étude des Lois Statistiques de l'Imagerie Cohérente," in *Rapport de* recherche, 2006D010, 2006.
- [7] L. Bombrun and J.-M. Beaulieu, "Fisher Distribution for Texture Modeling of Polarimetric SAR Data," *IEEE Geoscience and Remote Sensing Letters*, vol. 5, no. 3, pp. 512–516, July 2008.
- [8] L. Bombrun, J.-M. Beaulieu, G. Vasile, J.-P. Ovarlez, F. Pascal, and M. Gay, "Hierarchical Segmentation of Polarimetric SAR Images using Heterogeneous Clutter Models," in *Geoscience and Remote Sensing, IGARSS'09, Cape Town, South Africa*, 2009, vol. 3, pp. 5–8.
- [9] J.-M. Beaulieu and R. Touzi, "Segmentation of Textured Polarimetric SAR Scenes by Likelihood Approximation," *IEEE Transactions on Geoscience and Remote Sensing*, vol. 42, no. 10, pp. 2063–2072, October 2004.